Optics Letters

Terahertz modulation induced by filament interaction

Boqu He,[1] Junyi Nan,[1] Min Li,[2] Shuai Yuan,[2] and Heping Zeng[1,2,*]

[1]State Key Laboratory of Precision Spectroscopy, East China Normal University, Shanghai 200062, China
[2]Shanghai Key Laboratory of Modern Optical System, Engineering Research Center of Optical Instrument and System (Ministry of Education), School of Optical-Electrical and Computer Engineering, University of Shanghai for Science and Technology, Shanghai 200093, China
*Corresponding author: hpzeng@phy.ecnu.edu.cn

Received 13 December 2016; revised 25 January 2017; accepted 7 February 2017; posted 7 February 2017 (Doc. ID 282714); published 27 February 2017

We experimentally demonstrated that nonlinear filament interaction could spectrally modulate terahertz (THz) radiation generated from asymmetric two-color filaments. It was the spatial plasma density modulation in plasma channels that induced the THz spectral modulation. As a result of optical manipulation of electron density in the filamentary plasma gratings, the proportion of high-frequency THz spectra increased, while that of low-frequency THz spectra decreased, indicating that the increase of free electron density in the filamentary plasma grating brought about THz frequency upshifts.

OCIS codes: (300.6495) Spectroscopy, terahertz; (300.6380) Spectroscopy, modulation; (320.7120) Ultrafast phenomena.

https://doi.org/10.1364/OL.42.000967

Ultrafast laser filamentation has been extensively studied over the past two decades for its abundant applications in various fields such as THz generation [1], supercontinuum generation [2,3], remote sensing [4], and electric discharge control [5,6]. Filaments are typically observed as weakly ionized channels in the wake of laser pulse propagation, contributing to the dynamic balance of the Kerr focusing and plasma defocusing. Two crossing filaments have been proposed to remotely manipulate filamentation and nonlinear filament interactions [7–12]. In the interacting region of two laser pulses, filamentary interference gives rise to a plasma grating. The plasma grating has been used to enhance the generation of the third harmonic (TH) [10,13] and to excite atoms and molecules [11]. Interestingly, two-color filaments could be optically controlled by a single-color filament via noncollinear filament interaction, from which plasma gratings induced observable energy transfer [9]. It is well-known that THz generation is normally achieved with two-color laser filaments involving the fundamental-wave (FW) and its second harmonic (SH) pulses propagating in ambient air [14–17]. It has been previously demonstrated that the THz spectrum could be tuned by modification of the plasma density inside a single filament by changing the focal length [18]. Because the density in the plasma grating is periodically modulated, it is intriguing to investigate THz spectral modulation induced by nonlinear filament interactions.

As for THz radiation, the significant characterization is that the typical THz spectrum (0.1–10 THz) spans beyond the standard electromagnetic spectrum, which features distinctive fingerprints in numerous chemical and biological materials. Many THz spectroscopic applications require efficient modulation of the THz spectrum. However, most effort has been devoted to either electric field enhancement [19–24] or THz polarization control [25,26], while THz spectral modulation induced by the laser filament has so far been less explored. To our knowledge, related works in THz frequency modulation have been done either by using specific modulators to alter the existing THz radiation [27–29], or shaping the pump pulse profile in optical rectification technique different from THz generation induced by two-color filamentation [30].

In this Letter, we report on the experimental demonstration of all-optical THz spectral modulation induced by filamentary interference. The filamentary interference occurred in the case of two filaments with parallel and perpendicular polarizations, respectively. The experimental results indicated that the higher frequency components of the generated THz were enhanced, while the lower frequency components were suppressed. Our result experimentally supports that four-wave mixing and photocurrent effects contribute to THz generation driven by the asymmetric two-color field.

As illustrated in Fig. 1, a Ti:Sapphire laser system based on chirped-pulse-amplification was employed. The laser delivered pulses with 50 fs pulse duration, 800 nm central wavelength and 1 kHz repetition rate. The initial laser pulse with 2.2 mJ pulse energy was split into two parts with equal pulse energy. One part passed through a frequency-doubling crystal β-BBO (200 μm, I type) to generate SH pulses, which co-propagated with the FW pulse to form a asymmetric two-color field for THz generation. The other part (dubbed as the third pulse hereafter) was employed to interfere with the FW of the two-color pulses. All the pulses were focused by using lenses of 50 cm focal length. The polarization and pulse energy of the third pulse were adjusted with a half-wave plate and neutral density filters. The interacting filaments were precisely

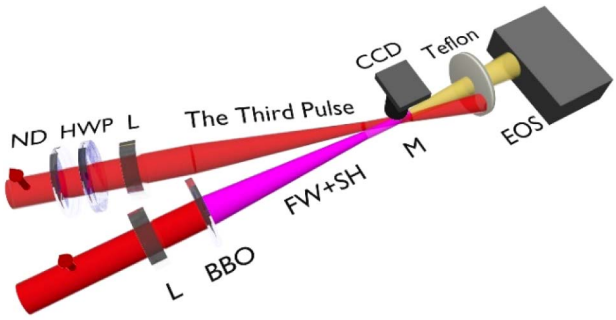

Fig. 1. Schematic diagram of THz modulation induced by the plasma grating formed via nonlinear interaction of two 800-nm laser pulses. ND: neutral density filters, HWP: half-wave plate, L: lens, BBO: β-barium borate Type-I crystal, CCD: charge coupled device, M: microscope, EOS: electric-optic sampling setup.

synchronized by the delay line in the third pulse path. The crossing angle of the FW and the third laser pulse was 5.5°. A microscope (10× microobjective) equipped with a CCD was applied on the top of the interacting filaments to record the fluorescence image of the plasma channels. The periodically aligned microstructures formed in the interaction region. An opaque Teflon plate was placed behind the filaments to block the visible laser and transmit the generated cone-like THz radiation [31,32]. The THz pulses were refocused on a 1.5-mm-thick ZnTe crystal by using a pair of off-axis parabolic mirrors with 101.6-mm effective focal length. The weak probe pulse leaked from the highly reflecting mirrors was combined with the generated THz via a Pellicle bean splitter, and then the THz wave was detected using an electric optical sampling method [33].

As shown in Figs. 2(a) and 2(b), the interference fringes of the plasma grating were captured when the FW and the third laser pulse had parallel and perpendicular polarizations, respectively. The spatial period of plasma grating Λ was measured to be about 8.1 μm at a crossing angle of 5.5°, which agrees with the calculated value of 8.3 μm determined by $\Lambda = \lambda_{FW}/[2\sin(\theta/2)]$, where λ_{FW} is the central wavelength of the FW pulse. So far, most experiments have considered only nonlinear interference of two filaments with parallel polarizations [7–11]. However, generation of transient plasma grating is also possible for two perpendicularly polarized interacting

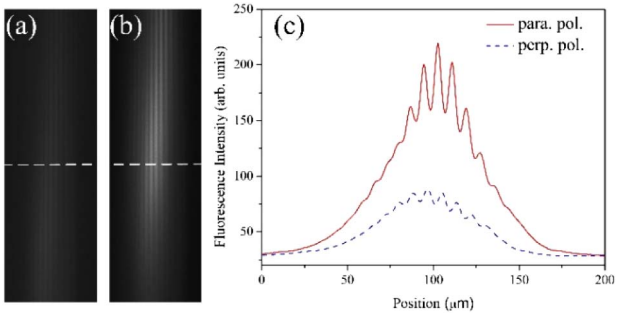

Fig. 2. Plasma grating formed by using two cross-overlapped pulses with perpendicular polarizations (a) and parallel polarizations (b). The fluorescence intensities of the plasma grating with different polarizations are shown in (c).

pulses. As shown in Fig. 2(c), the fringes for parallel polarizations had better contrast ratio and higher plasma fluorescence intensity than those for the perpendicular one. The plasma grating fringes for perpendicular polarization should be attributed to nonlinear polarization rotation induced by the birefringence. The isotropic medium was turned into anisotropic in the intense intersection region. The FW pulse induced a stronger third-order susceptibility parallel to the laser field than that perpendicular to the laser field [34]. As a result, the third pulse experiences two different extra refraction indices by means of cross-phase modulation, leading to a phase difference between the parallel and perpendicular components. The accumulated phase difference along the intersection region rotates the pulse polarization from linear to elliptical. And the nitrogen fluorescence for different polarizations indicated that the multiphotoionization-induced plasma density was periodically modulated in space, resulting in spatial modulation of the refractive index. The ionization process is proportional to the laser intensity in the interacting region. It is inferred that the local laser intensity for parallel polarization is stronger than that for the perpendicular one. The THz spectra could be modulated by this kind of nonlinear interference.

In our experiments, the FW of two-color filaments was *s*-polarized, and the polarization of the third laser pulse for plasma grating generation was initially rotated to be parallel to the FW and gradually switched to perpendicular. The THz waveforms measured under three typical situations are shown in Fig. 3(a). Compared with the THz electric field without plasma grating, the amplitudes of THz electric field were decreased as influenced by the preformed plasma grating. When two parallel polarized laser pulses formed the plasma grating, THz electric field amplitude was even lower than that influenced by plasma grating with perpendicularly polarized laser pulses. Recently, Andreeva *et al.* [35] pointed out that both four-wave mixing from neutrals and plasma photocurrent from tunneling ionization contribute to the two-color filament induced THz generation. Moreover, the contribution from neutrals by four-wave mixing is much weaker, and it occurs at higher frequencies than the distinctive plasma with lower frequency contribution. Hence, the photocurrent effect plays a dominating role in the THz field amplitude [35]. In this model, free electrons are stripped off from the nucleus after tunneling ionization by an asymmetric two-color field, which are subsequently accelerated by the residual laser field to form nonvanishing transverse current, producing THz radiation. As for influence of the plasma grating, energy transfer should be taken into account. For sufficiently small incident angles in our experimental setup, the Bragg diffraction of SH pulse is governed by $\Lambda\sin(\varphi) = m\lambda_{SH}$, where λ_{SH} is the central wavelength of the incident SH pulse, φ is the angle between the incident pulse and the axis of the preformed plasma grating. The SH pulse was collinear with the FW, thus, $\varphi = \theta/2$; this meets the requirement for the first-order Bragg diffraction, leading to the tight guiding of the SH. As demonstrated in previous experiments [9], part of the SH energy was transferred to the bisector direction of the interacting region between the two-color and the third laser filaments. It is well-known that the THz electric field is dependent on the intensity ratio of the two-color field [36]. Hence, the previous appropriate intensity ratio was detrimentally altered because of energy transfer, leading to lower THz conversion efficiency.

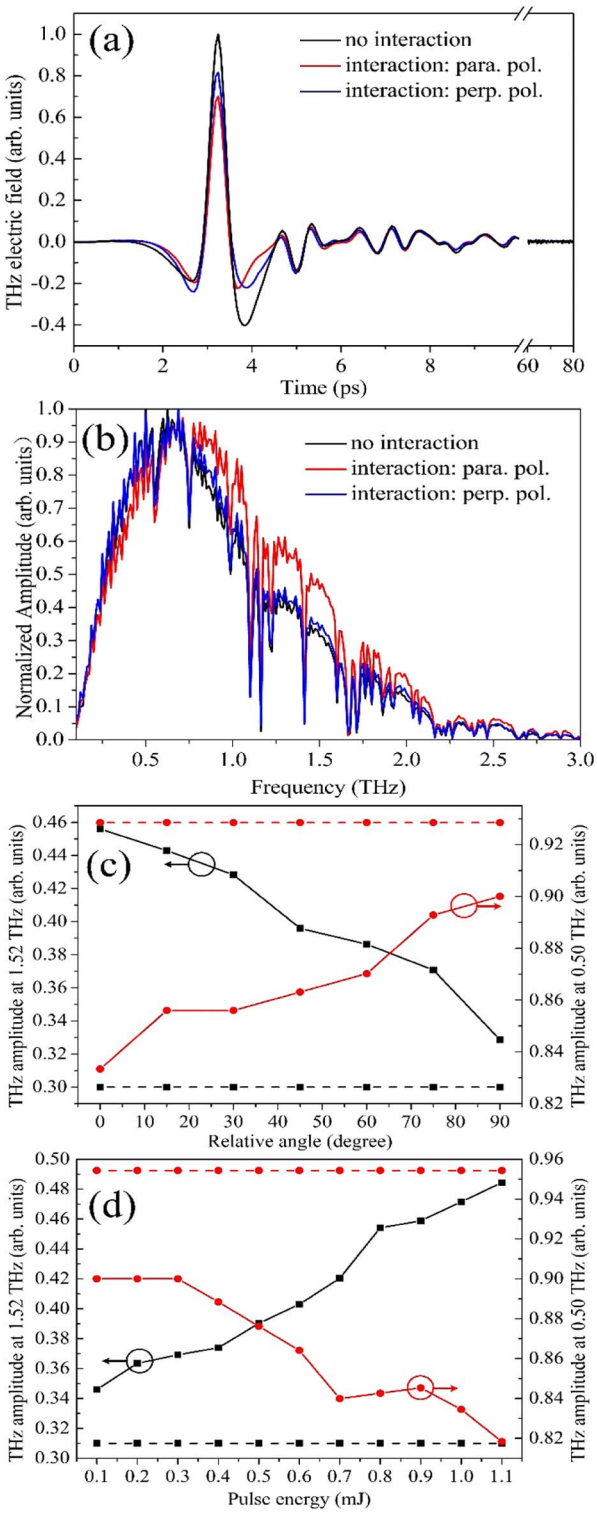

Fig. 3. THz electric fields (a) and the corresponding normalized spectra (b) generated by two-color filaments without plasma grating (black curve), with plasma grating formed by parallel-polarized (red curve) and perpendicularly polarized (blue curve) filaments, respectively. The dependence of the THz amplitude at 1.52 THz (black-squared solid curves) and 0.50 THz (red-circled solid curves) on the relative angle (c) and pulse energy (d) of the input third pulse to form plasma grating. The relative angle is the intersection angle between polarization directions of the FW and the third pulses. Dashed line indicates signals measured without plasma grating.

We demonstrated the dependence of THz amplitudes of different frequencies on the relative angle of polarization directions and the pulse energy of the third laser pulse. In the normalized THz spectra Fourier-transformed from the time domain waveforms, the three typical spectra from 0.1 to 3 THz were shown in Fig. 3(b). Influenced by interference with parallel polarized pulses, the proportion of high frequency components increased and that of low frequency components decreased. Subsequently, we chose amplitudes at 1.52 and 0.50 THz in the normalized THz spectra to depict high frequency (0.75–3 THz) and low frequency (0.1–0.75 THz) variation trend as shown in Fig. 3(c). When the relative angle varies from 0° to 90°, i.e., parallel polarizations gradually changing to perpendicular polarizations, the amplitude at 1.52 THz keeps decreasing and amplitude at 0.50 THz keeps increasing. And using the highest pulse energy of 1.1 mJ in our experiment, maximal modulation at 1.52 THz and minimal modulation at 0.50 THz were observed in Fig. 3(d). It has been experimentally reported [35] that frequency below 0.75 THz is due to the photocurrent induced by the plasma, reaching a peak frequency at 0.75 THz for typical free-electron density $N_e \approx 7 \times 10^{15}$ cm^{-3}. It is consistent with our peak frequency of approximately 0.75 THz as shown in Fig. 3(b). And it could be interpreted that frequency from 0.75 to 3 THz is due to four-wave mixing contribution. In the perspective of photocurrent mechanism, the generated THz frequency is related to the free-electron density for plasma determined by $\nu = \omega/2\pi = (N_e e^2/m\varepsilon_0)^{1/2}/2\pi$, where N_e is the free-electron density [1]. The electron density was demonstrated to increase with the focused peak intensity before saturation near the clamped peak intensity within the plasma channel [37]. Nonlinear interaction of two femtosecond filaments could generate plasma gratings that exceed the clamped intensity level for free electron generation [17]. With two interacting laser pulses parallel polarized, the peak intensity in the plasma grating is greater compared to the plasma grating with perpendicularly polarized pulses.

Moreover, greater electron density was generated in plasma gratings of parallel polarized pulses than perpendicularly polarized pulses. Due to the increasing free electron density, electron frequency was shifted to higher frequency, decreasing the amplitudes of lower THz frequency components.

In the perspective of four-wave mixing mechanism, it benefits from plasma-enhanced third-order susceptibility, leading to the increase of the higher THz frequency component. The third-order susceptibility enhancement could be validated by testing the third harmonic intensity [38]. In our experiment, the TH spectrum at the end of two-color filaments was separated by using one fused silica prism and detected with a high-resolution spectrometer. Figure 4 compares the TH spectra surrounding the central wavelength of 266 nm with and without the third infrared laser pulse to preform plasma grating. Influenced by plasma grating preformed with parallel polarized pulses, the TH amplitude was remarkably stronger. TH intensity slightly increased under the influence of plasma grating preformed by perpendicular polarization. The increasing plasma density for parallel polarized plasma grating improved the third-order susceptibility, bringing about enhanced TH intensity. The relationship between the TH and THz spectra could be explained as follows: the enhanced TH spectra could be partially attributed to the enhanced third-order susceptibility.

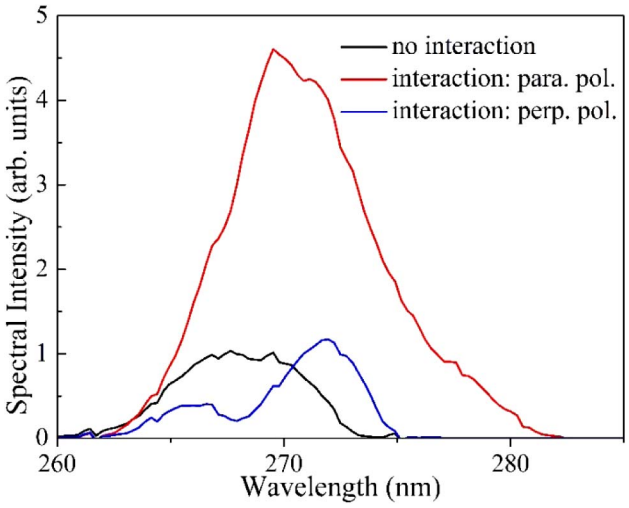

Fig. 4. Third harmonic spectra with and without plasma grating.

Because rectification by four-wave mixing contributes to high frequency components of THz radiation, TH spectra could be a hint of the corresponding THz ones. The results roughly matched with the corresponding THz spectra, which justified the important role of four-wave mixing in the two-color filament induced THz generation.

In conclusion, we demonstrated an all-optical method to modulate the THz spectrum as electron density was changed by filamentary interference. The proportion of high frequency components increased, while that of low frequency components decreased in the THz spectra. Our experiment supports the hypothesis that both four-wave mixing and photocurrent mechanisms contribute to THz generation driven by the asymmetric two-color field, which agrees with the theory. Both contributions could be modulated by nonlinear filament interaction with a third pulse. The high frequency above 0.75 THz covers most of the crystalline phonon vibrations, torsional deformations, and intermolecular bonding. It provides unique sensitivity to lattice structure enabling qualitative and quantitative analysis of crystalline and amorphous materials. This kind of approach may benefit applications in the field of THz spectroscopy.

Funding. Science and Technology Commission of Shanghai Municipality (STCSM) (14JC1401600); National Natural Science Foundation of China (NSFC) (11434005, 11561121003, 61505106); National Key Scientific Instrument Project (2012YQ150092).

REFERENCES

1. C. D'Amico, A. Houard, M. Franco, B. Prade, A. Mysyrowicz, A. Couairon, and V. T. Tikhonchuk, Phys. Rev. Lett. **98**, 235002 (2007).
2. H. Cai, J. Wu, X. Bai, H. Pan, and H. Zeng, Opt. Lett. **35**, 49 (2010).
3. E. Goulielmakis, S. Koehler, B. Reiter, M. Schultze, A. J. Verhoef, E. E. Serebryannikov, A. M. Zheltikov, and F. Krausz, Opt. Lett. **33**, 1407 (2008).
4. J. Kasparian, M. Rodriguez, G. Méjean, J. Yu, E. Salmon, H. Wille, R. Bourayou, S. Frey, Y. B. André, A. Mysyrowicz, R. Sauerbrey, J. P. Wolf, and L. Wöste, Science **301**, 61 (2003).
5. J. Kasparian, R. Ackermann, Y. B. André, G. Méchain, G. Méjean, B. Prade, P. Rohwetter, E. Salmon, K. Stelmaszczyk, J. Yu, A. Mysyrowicz, R. Sauerbrey, L. Wöste, and J.-P. Wolf, Opt. Express **16**, 5757 (2008).
6. E. Schubert, D. Mongin, J. Kasparian, and J. P. Wolf, Opt. Express **23**, 28640 (2015).
7. A. C. Bernstein, M. McCormick, G. M. Dyer, J. C. Sanders, and T. Ditmire, Phys. Rev. Lett. **102**, 123902 (2009).
8. Y. Liu, M. Durand, S. Chen, A. Houard, B. Prade, B. Forestier, and A. Mysyrowicz, Phys. Rev. Lett. **105**, 055003 (2010).
9. X. Yang, J. Wu, Y. Tong, L. Ding, Z. Xu, and H. Zeng, Appl. Phys. Lett. **97**, 071108 (2010).
10. X. Yang, J. Wu, Y. Peng, Y. Tong, S. Yuan, L. Ding, Z. Xu, and H. Zeng, Appl. Phys. Lett. **95**, 111103 (2009).
11. X. Yang, J. Wu, Y. Peng, Y. Tong, P. Lu, L. Ding, Z. Xu, and H. Zeng, Opt. Lett. **34**, 3806 (2009).
12. L. Shi, W. Li, Y. Wang, X. Lu, L. Ding, and H. Zeng, Phys. Rev. Lett. **107**, 095004 (2011).
13. Y. Liu, M. Durand, A. Houard, B. Forestier, A. Couairon, and A. Mysyrowicz, Opt. Commun. **284**, 4706 (2011).
14. M. Kress, T. Löffler, S. Eden, M. Thomson, and H. G. Roskos, Opt. Lett. **29**, 1120 (2004).
15. D. Kuk, Y. J. Yoo, E. W. Rosenthal, N. Jhajj, H. M. Milchberg, and K. Y. Kim, Appl. Phys. Lett. **108**, 121106 (2016).
16. M. Li, W. Li, Y. Shi, P. Lu, H. Pan, and H. Zeng, Appl. Phys. Lett. **101**, 161104 (2012).
17. K. Y. Kim, J. H. Glownia, A. J. Taylor, and G. Rodriguez, Opt. Express **15**, 4577 (2007).
18. Y. Chen, T. J. Wang, C. Marceau, F. Théberge, M. Châteauneuf, J. Dubois, O. Kosareva, and S. L. Chin, Appl. Phys. Lett. **95**, 101101 (2009).
19. J. Zhao, L. Guo, W. Chu, B. Zeng, H. Gao, Y. Cheng, and W. Liu, Opt. Lett. **40**, 3838 (2015).
20. J. M. Manceau, M. Massaouti, and S. Tzortzakis, Opt. Lett. **35**, 2424 (2010).
21. Y. Liu, A. Houard, B. Prade, S. Akturk, A. Mysyrowicz, and V. T. Tikhonchuk, Phys. Rev. Lett. **99**, 135002 (2007).
22. X. Xie, J. Xu, J. Dai, and X.-C. Zhang, Appl. Phys. Lett. **90**, 141104 (2007).
23. Y. Minami, M. Nakajima, and T. Suemoto, Phys. Rev. A **83**, 023828 (2011).
24. C. Meng, W. Chen, X. Wang, Z. Lü, Y. Huang, J. Liu, D. Zhang, Z. Zhao, and J. Yuan, Appl. Phys. Lett. **109**, 131105 (2016).
25. M. Li, H. Pan, Y. Tong, C. Chen, Y. Shi, J. Wu, and H. Zeng, Opt. Lett. **36**, 3633 (2011).
26. J. M. Manceau, M. Massaouti, and S. Tzortzakis, Opt. Express **18**, 18894 (2010).
27. M. Rahm, J.-S. Li, and W. J. Padilla, J. Infrared Millim. Terahertz Waves **34**, 1 (2013).
28. S. Zarei and M. Jarrahi, in *IEEE Photonics Society Winter Topicals Meeting Series* (IEEE, 2010), p. 30.
29. S. F. Shi, B. Zeng, H. L. Han, X. Hong, H. Z. Tsai, H. S. Jung, A. Zettl, M. F. Crommie, and F. Wang, Nano Lett. **15**, 372 (2015).
30. C. D'Amico, M. Tondusson, J. Degert, and E. Freysz, Opt. Express **17**, 592 (2009).
31. K. Pernille, C. S. Andrew, I. Krzysztof, and J. Peter Uhd, New J. Phys. **15**, 075012 (2013).
32. A. Gorodetsky, A. D. Koulouklidis, M. Massaouti, and S. Tzortzakis, Phys. Rev. A **89**, 033838 (2014).
33. Q. Wu and X. C. Zhang, Appl. Phys. Lett. **67**, 3523 (1995).
34. S. L. Chin, T. J. Wang, C. Marceau, J. Wu, J. S. Liu, O. Kosareva, N. Panov, Y. P. Chen, J. F. Daigle, S. Yuan, A. Azarm, W. W. Liu, T. Seideman, H. P. Zeng, M. Richardson, R. Li, and Z. Z. Xu, Laser Phys. **22**, 1 (2012).
35. V. A. Andreeva, O. G. Kosareva, N. A. Panov, D. E. Shipilo, P. M. Solyankin, M. N. Esaulkov, P. González de Alaiza Martínez, A. P. Shkurinov, V. A. Makarov, L. Bergé, and S. L. Chin, Phys. Rev. Lett. **116**, 063902 (2016).
36. C. Lu, S. Zhang, Y. Yao, S. Xu, T. Jia, J. Ding, and Z. Sun, RSC Adv. **5**, 1485 (2015).
37. A. Couairon and A. Mysyrowicz, Phys. Rep. **441**, 47 (2007).
38. S. Suntsov, D. Abdollahpour, D. G. Papazoglou, and S. Tzortzakis, Phys. Rev. A **81**, 033817 (2010).